Stop-and-Wait: Discover Aggregation Effect Based on Private Car Trajectory Data

Dong Wang, *Member, IEEE*, Jiaojiao Fan, Zhu Xiao, *Member, IEEE*, Hongbo Jiang, *Senior Member, IEEE*, Hongyang Chen, *Senior Member, IEEE*, Fanzi Zeng, and Keqin Li, *Fellow, IEEE*

***Abstract*— Private cars, a class of small motor vehicles usually registered by an individual for personal use, constitute the vast majority of city automobiles and hence significantly affect urban traffic. In particular, private cars tend to stop-and-wait (SAW) in specific regions during daily driving. This SAW behavior produces a spatiotemporal aggregation effect, which facilitates the formation of urban hot zones. In this paper, we investigate the SAW behavior and aggregation effect based on large-scale private car trajectory data. Specifically, motivated by the first law of geography, we leverage the kernel density estimation (KDE) method and extend it to three dimensions to capture the density distribution of the SAW data. Furthermore, according to the inherent relationship between the present SAW density and future SAW aggregation, we propose a 3D-KDE-based prediction model to characterize the dynamic spatiotemporal aggregation effect. In addition, we design a modified inertia weight particle swarm optimization (MIW-PSO) algorithm to determine the optimal weight coefficients and to avoid local optima during SAW prediction. Extensive experiments based on real-world private car SAW data validate the effectiveness of our method for discovering dynamic aggregation effects, therein outperforming the current methods in terms of the Kullback-Leibler (KL) divergence, mean absolute error (MAE), and root mean square error (RMSE). To the best of the authors' knowledge, our work is the first to utilize private car trajectory data to study the aggregation effect in urban environments, thereby being able to provide new insight into the study of traffic management and the evolution of urban traffic.**

***Index Terms*— Aggregation effect, private car, stop-and-wait (SAW), kernel density estimation, trajectory data.**

Manuscript received January 23, 2018; revised August 13, 2018; accepted October 21, 2018. Date of publication November 12, 2018; date of current version October 2, 2019. This work was supported in part by the National Natural Science Foundation of China under Grant 61502162, Grant 61702175, and Grant 61772184, in part by the Fund of the State Key Laboratory of Geoinformation Engineering under Grant SKLGIE2016-M-4-2, in part by the Hunan Natural Science Foundation of China under Grant 2018JJ2059, in part by the Key R & D Project of Hunan Province of China under Grant 2018GK2014, and in part by the Open Fund of the State Key Laboratory of Integrated Services Networks under Grant ISN17-14. The Associate Editor for this paper was I. Papamichail. *(Corresponding author: Zhu Xiao.)*

D. Wang and Z. Xiao are with the College of Computer Science and Electronic Engineering, Hunan University, Changsha 410082, China, and also with the State Key Laboratory of Integrated Service Networks, Xidian University, Xi'an 710071, China (e-mail: wangd@hnu.edu.cn; zhxiao@hnu.edu.cn).

J. Fan, H. Jiang, and F. Zeng are with the College of Computer Science and Electronic Engineering, Hunan University, Changsha 410082, China (e-mail: fanjiaojiao@hnu.edu.cn; hongbojiang2004@gmail.com; zengfanzi@hnu.edu.cn).

H. Chen is with the Institute of Industrial Science, The University of Tokyo, Tokyo 153-8505, Japan (e-mail: dr.h.chen@ieee.org).

K. Li is with the College of Computer Science and Electronic Engineering, Hunan University, Changsha 410082, China, and also with the Department of Computer Science, The State University of New York, New Paltz, NY 12561 USA (e-mail: lik@newpaltz.edu).

Digital Object Identifier 10.1109/TITS.2018.2878253

I. Introduction

A. Background and Motivation

In recent years, the ever-increasing number of automobiles has exerted tremendous pressure through a series of problems facing modern cities such as municipal transportation services, traffic management and environmental protection [1]. Meanwhile, the large numbers of vehicles driving along urban road networks produce a huge volume of vehicular trajectory data. Therefore, collecting vehicle trajectory and analyzing such information provide a promising solution to alleviating traffic jams and improving transport services [2], [3]. Moreover, it creates new opportunities for understanding people's travel behaviors and the evolution of urban traffic [4].

During daily driving, people stop their car when they reach certain locations [5], which are normally preset destinations such as locations of employment, shopping areas, residential areas, and frequented public areas. In addition, cars stay and wait for certain periods of time since people will spend time at these places with their own purposes before they come back to their car and drive away. This travel behavior can be referred to as stop-and-wait (SAW) and can be observed when studying the SAW points originating from the trajectory data. In other words, the so-called SAW behavior directly reflects people's travel demands because people need to stop their car at certain locations and spend time at nearby locations to conduct their activities. Therefore, people driving in the city exhibit a specific SAW behavior and hence generate aggregation effects [6], which in turn lead to a form of hot zones in urban environments. Further, the SAW data offer valuable information for understanding the development of urban traffic, thereby being capable of benefiting trajectory data mining and urban computing [7], [8].

Note that for urban vehicles, one fact is that the great majority of private cars, i.e., a class of small motor vehicles usually registered by an individual and for personal use, constitute the vast majority of city automobiles. For instance, with the further industrialization and urbanization of China, the number of automobiles reached 194 million by the end of 2016, more than 80 percent of which are private cars [9]. Therefore, this large number of private cars contributes remarkably to urban problems such as traffic congestion, urban energy consumption and the emissions of polluting gases [8]. More importantly, private cars drive with a clear purpose based on the personal travel demands and generate distinctly different SAW points compared with the other two types of

vehicles in a city [10]: buses and taxis. Specifically, buses are designed to carry many passengers; they move along a predefined route on a preset time schedule and stop at a fixed location, i.e., bus stations, which are normally determined by public transportation service providers. Hence, the SAW behaviors of buses are mostly steady both in terms of travel time and stopping location. Taxis drive in a city and provide non-shared rides for a single passenger or small group of passengers, the SAW behaviors of which are concentrated at drop-off/pick-up passengers. Unlike buses, the SAW locations for taxis are completely determined by the passenger, usually being random and relying on the travel demands of the passengers for a personal trip. The driving of private cars is based on personal travel needs; in most cases, it directly reflects the individual travel demands for people with long-term use of the vehicle, who are likely the private car owners or their family members. Moreover, private cars driving in the city exhibit a certain degree of regularity [11], namely, their travels are often concentrated in specified areas, such as residential, workplace and hot spots in the city, which in turn generate aggregation effects. In other words, large numbers of vehicles, the majority of which being private cars, drive to the same areas, and their SAW behaviors lead to the formation of urban hot zones. In this context, the SAW behaviors obtained from private car trajectory data best reflect the spatiotemporal aggregation effect during the evolution of urban traffic.

Currently, research using the trajectory data of private cars is scarce, especially concerning the SAW behavior. In this paper, we propose analysis of the characteristics of SAW behaviors hidden in large-scale trajectory data collected from private cars and to discover the spatiotemporal aggregation effect. In particular, this study attempts to provide new thinking to reveal human travel patterns and optimize the design of traffic management and urban computing systems.

B. Related Work

The analysis of trajectory data of vehicles and learning knowledge from the trajectory information have attracted substantial attention in existing studies. The authors of [12] use GPS trajectories generated by over 32,000 taxis in Beijing over 47 days to compute the travel speed of each road segment. Combining with the speed and traffic volume of the road segment, they compute the real-time fuel consumption and exhaust emissions of vehicles running on the road network. In [13], the authors utilize transit smart card data covering Oyster transactions across all public transport modes, including bus and rail, to measure travel behaviors. In [14], the authors investigate the geocast strategy in bus-based VANETs and present a geocast routing mechanism with historical bus trajectories. In [15], the authors propose the headway adherence as an indicator of regularity and use automatic vehicle location (AVL) data to analyze the travel mode in a bus transit network. A novel approach named T-CONV is applied to model multi-scale trajectories collected from 442 taxis for a year as two-dimensional images toward achieving precise prediction [16]. The authors in [17] utilize thousands of buses equipped with GPS to generate a tremendous amount of bus data and propose a Bus Trajectory-based Congestion Identification (BTCI) framework to explore the anomalous traffic status. In summary, current studies on trajectory data focus on floating cars or probe vehicles [10] and rarely consider private cars and their SAW behaviors.

An aggregation effect is generated in areas where the concentration of points inside is significantly high, which can reveal valuable information about the underlying environments such as road-way networks, traffic volumes and human activities [18]. In urban areas, the aggregation effect of vehicles has important social and application value [6], [7], [19] since it can be used for identifying frequent patterns, mining urban hotspots, reducing traffic congestion, etc. In [20], the authors present a three-in-one trajectory prediction method for implementing region-of-interest (ROI) discovery with 8000 moving objects on real-world transportation networks in Chengdu and in the U.S. states of New York and Kansas. The authors in [21] propose a Density-Based Hierarchical CLUStering (DBH-CLUS) method to identify pick-up/drop-off hotspots from 12,000 taxis during 3-month period. In [22], the authors present a combination Voronoi model and Mobile Mapping System (MMS) to update the POIs in Xicheng District, Beijing. However, these methods may generate false positive hotspots since they do not consider the relevance of the geographical location. Recently, researchers have proposed visualization techniques to drive analysis of aggregation-like features of trajectory data. In [23], the authors propose an interactive framework to address the problem of billboard location selection via designing a novel visualization-driven data mining model. To achieve this, the authors add a heatmap layer based on Google Maps API to conduct visual analytics with 3,501 taxis, over 230,000 road network data records and 154,633 POI data records. The authors in [24] propose an interactive system for visual analysis to extract urban traffic congestion from taxi trajectories, in which the traffic speed on each road segment is computed and traffic jam events are automatically detected. This indicates the feasibility of low-speed trajectory data that are more suitable for the analysis of traffic congestion. There is a connection between these methods and our study of the aggregation effect. Specifically, with the concept of SAW, we emphasize that people stop their car at certain areas (such as places of work, shopping zones, and residential regions) and spend time performing their activities. The objective of our study is to discover the spatiotemporal aggregation effect based on the dynamic SAW density since the SAW behavior of private cars directly reflects people's travel demands, thereby leading to the aggregation effect.

C. Contributions

In this work, we focus on investigating the SAW behavior and discovering the aggregation effect based on studying the private car trajectory big data. To the best of the authors' knowledge, our work is the first to utilize the trajectory information obtained from private cars to study the aggregation effect in urban environments, thereby also providing a new perspective for investigating traffic management and urban planning. The trajectory data are collected by a low-cost and user-friendly onboard device, which is introduced in Section IV-A. The collected private car trajectory datasets

show the characteristics of the spatiotemporal aggregation. According to the first law of geography [25], the spatiotemporal aggregation effect can be explained as follows. *i*) The SAW points retrieved from the private car trajectory data for a specified urban area are related to each other. *ii*) Closer SAW points are more strongly related than are more distant points. This significantly contributes to the formation of hot zones in urban environments, in which the vehicle density is gradually increasing from the edge to the center of the hot zones. Inspired by this, we leverage the Kernel Density Estimation method [26] and extend it to three dimensions (3D-KDE) to characterize the dynamic density distribution of SAW. We then design a prediction model based on 3D-KDE to discover the inherent spatiotemporal aggregation effect. Note that the SAW density of the current day can be expressed by historical days of the current week and the current day of the previous week with corresponding weights. However, it is a delicate task to find proper weights for the prediction of the future SAW aggregation by exploiting the previous trajectory data. To this end, we design a modified inertia weight particle swarm optimization (MIW-PSO) method to determine the optimal weight coefficients and avoid local optima.

To validate the performance of our method, we conduct experiments based on the real-world private car trajectory data. Large volumes of SAW data collected from two cities in five weeks are used as the experiment dataset. According to the experimental results, we clearly observe the formation and disappearance of the dynamic aggregation effect. This reveals that the spatiotemporal features of the SAW data are particularly helpful for understanding the time-varying aggregation effect. Moreover, the results demonstrate that our proposed method outperforms current methods in terms of the KL divergence, MAE and RMSE.

The remainder of this paper is organized as follows. In Section II, we present an overview of the proposed method. The details of the proposed method are presented in Section III. Section IV gives the experimental data and results. Finally, Section V concludes the paper.

II. Method Overview

To investigate the aggregation effect, we propose a learning strategy to predict the SAW density based on the private car trajectory data in urban environments, the structure of which is given in Fig. 1. Let S_u^d denote the SAW data for the d-th day on the u-th week, where $S = \{(x_i, y_i, t_i)\}_{i=1,\ldots,n}$, with n being the number of SAW points; x_i and y_i denote the latitude and longitude of the i-th SAW point, respectively; and t_i is the timestamp for (x_i, y_i).

Our goal is to obtain the predicted density distribution for S_u^{d+1}, namely, $\hat{P}_u^{d+1}$, by learning from the historical SAW data. We use a total of T days of historical SAW data to predict the future density distribution. To achieve this, we construct a 3D-KDE model wherein the historical SAW data sequence S, i.e., $\left\{S_u^d, S_u^{d-1}, \ldots, S_u^{d-(T-2)}, S_{u-1}^{d+1}\right\}$, is taken as Input 1 (see in Fig. 1) and used to train the model. Then, we obtain the corresponding output of the 3D-KDE model, namely, the density distributions P, which

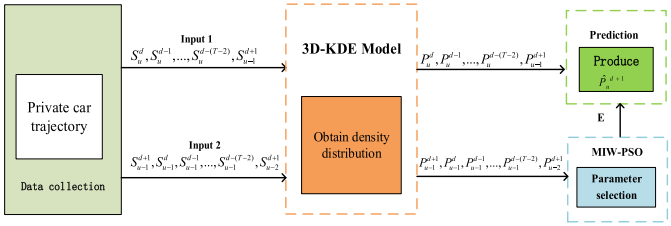

Fig. 1. Block diagram of SAW density prediction.

can be expressed by $\left\{P_u^d, P_u^{d-1}, \ldots, P_u^{d-(T-2)}, P_{u-1}^{d+1}\right\}$. Apart from the historical SAW data, the predicted $\hat{P}_u^{d+1}$ is highly related to the weight coefficients $\mathrm{E} = \left\{e_{0,\ldots,} \ e_{T-1}\right\}$, which are used to evaluate the impact of each day's SAW data in the training sequence. To achieve the optimal E, we use the SAW data of the previous week to conduct the parameter selection. In detail, as shown in Fig. 1, Input 2 is denoted by $\left\{S_{u-1}^{d+1}, S_{u-1}^d, S_{u-1}^{d-1}, \ldots, S_{u-1}^{d-(T-2)}, S_{u-2}^{d+1}\right\}$, where $S_{u-1}^d, S_{u-1}^{d-1}, \ldots, S_{u-1}^{d-(T-2)}, S_{u-2}^{d+1}$ can be used to obtain the predicted SAW density distribution $\hat{P}_{u-1}^{d+1}$ with the weight parameter, and the true SAW data S_{u-1}^{d+1} can be used to generate the true density distribution P_{u-1}^{d+1}. During the parameter training process, we use the MIW-PSO method to select the optimal E, which is used to guarantee that $\hat{P}_{u-1}^{d+1}$ is sufficiently close to the true P_{u-1}^{d+1} based on the output $\left\{P_{u-1}^d, P_{u-1}^{d-1}, \ldots, P_{u-1}^{d-(T-2)}, P_{u-2}^{d+1}\right\}$ of the 3D-KDE model. The details of the proposed approach are presented in the next section.

III. The Proposed Algorithm for SAW Discovery

A. 3D Kernel Density Estimation

The proposed approach based on Three-Dimensional Kernel Density Estimation (3D-KDE) is designed to identify the spatiotemporal correlation in the SAW data, which can be used to generate a density surface from a set of SAW points located in a geographic space at any time. The approach can be implemented by bandwidth selection and kernel functions. Generalized SAW data in S containing three basic elements, (x, y, t), namely, the latitude and longitude of the SAW points and the timestamp. For each voxel given the coordinates $(\upsilon x, \upsilon y, \upsilon t)$ in our research 3D region, its density is estimated based on the surrounding points (x_j, y_j, t_j) in S, the transform formula can be expressed as

$$f(\upsilon x, \upsilon y, \upsilon t) = \frac{1}{n h_s^2 h_t} \sum_{j|d_j<h_s, t_j<h_t} k_s\left(\frac{\upsilon x - x_j}{h_s}, \frac{\upsilon y - y_j}{h_s}\right) \times k_t\left(\frac{\upsilon t - t_j}{h_t}\right), \quad (1)$$

where f is the SAW density estimate function at the location $(\upsilon x, \upsilon y, \upsilon t)$, n is the number of SAW points, and h_s denotes the spatial bandwidth that forms a circle, whereby the temporal bandwidth h_t extends the circle to a cylinder based on the spatiotemporal orthogonal relationship, as shown in Fig. 2. The spatial and temporal distances between the voxel and SAW points are given by d_j and t_j. More importantly, the Gaussian

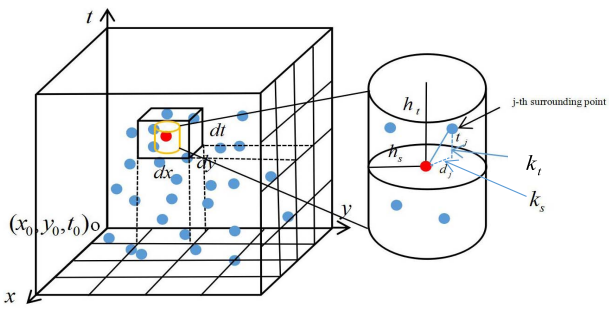

Fig. 2. The computation of 3D-KDE in a space-time cube.

kernel is used in defining the functions k_s and k_t. Based on Silvermans' rule of thumb, the computational formula of the bandwidth selection for the Gaussian kernel can be written as follows [27]:

$$\begin{cases} h_s = \left(\dfrac{4\widehat{\sigma_1}^5}{3n}\right)^{\frac{1}{5}} \\ h_t = \left(\dfrac{4\widehat{\sigma_2}^5}{3n}\right)^{\frac{1}{5}}, \end{cases} \tag{2}$$

where $\widehat{\sigma_1}$ and $\widehat{\sigma_2}$ are the standard deviation of the SAW data in the space and time dimension, respectively.

According to the above analysis, the SAW points of a given day can be used to build a density distribution model based on the 3D-KDE method, namely, P. Then, we can predict the SAW density distribution $\hat{P}$ in the future by combining with the historical density distributions and the corresponding weight E.

To improve the comparability, we extract some fixed sampling voxels using an appropriate set of dx,dy,dt to divide our research 3D region into $n_a \times n_b \times n_c$ space-time cubes, as shown in Fig. 2. Therefore, the value of the center point in the cube (see the red voxel in Fig. 2) can be computed by (3) based on (1) and (2):

$$P_{a,b,c}(x_{ma}, y_{mb}, t_{mc}) = f\left(x_0 + \frac{2a-1}{2} \times dx, y_0 + \frac{2b-1}{2} \times dy, t_0 + \frac{2c-1}{2} \times dt\right) \tag{3}$$

where $P_{a,b,c}$ represents the SAW density estimation for the space-time cube in (a, b, c) from the 3D region, $(x_{ma}, y_{mb}, t_{mc})|_{a=1,\ldots,n_a, b=1,\ldots,n_b, c=1,\ldots,n_c}$ denotes the coordinates of the space-time cube center, and (x_0, y_0, t_0) represents the starting point.

B. Optimization of Parameter Selection in SAW Density Prediction

To achieve the optimal E, we use the SAW density distributions of the last week to forecast the known density distribution through the weight parameter training. In detail, let $E = \{e_{0,\ldots,} \ e_{T-1}\} \in [0, 1]$ denote the vector of weight coefficients; e_0 represents the weight value of P_{u-2}^{d+1}; and the remaining $e_1, e_2, \ldots, e_{T-1}$ are the corresponding weights of $P_{u-1}^{k}|_{k=d,d-1,\ldots,d-(T-2)}$. Then, the predicted distribution can be expressed by

$$\hat{P}_{u-1}^{d+1} = e_0 \times P_{u-2}^{d+1} + \sum_{i=1}^{T-1} e_i \times P_{u-1}^{d-i+1}. \tag{4}$$

Selecting the optimal E requires a huge amount of computing work, especially for multidimensional and multimodal data. To obtain the weights with high precision and fast convergence, we design the MIW-PSO method to achieve the appropriate E to minimize the differences between the true and predicted SAW density distributions. The proposed MIW-PSO method prevents the algorithm from falling into a local optimum and achieves fast convergence. The search space is shaped by all possible values from the T-dimensional vector within the range [0, 1]. The m-th particle of the swarm can be denoted by $E_m = (e_{m_0}, e_{m_1}, \ldots, e_{m_{T-1}})$ to represent its position change. The $lbp_m = (lbp_{m_0}, lbp_{m_1}, \ldots, lbp_{m_{T-1}})$ is used to record the best position of the m-th particle; the best position of all particles is $gbp_g = (gbp_{g_0}, gbp_{g_1}, \ldots, gbp_{g_{T-1}})$. Similarly, the velocity can be described by another T-dimensional vector $V_m = (v_{m_0}, v_{m_1,\ldots,} \ v_{m_{T-1}})$. According to [28], the update formula of the velocity and position at the k-th iteration of each particle can be written as

$$V_{m_t}^{k+1} = w_m^k \ V_{m_t}^k + C^1 R^1 \left(lbp_{m_t}^k - E_{m_t}^k\right) + C^2 R^2 \left(gbp_{g_t} - E_{m_t}^k\right), \tag{5}$$

$$E_{m_t}^{k+1} = E_{m_t}^k + V_{m_t}^{k+1}, \tag{6}$$

where m denotes the m-th particle of the swarm and $m = 1, \ldots, N_{size}$ and N_{size} is the total number of particles. The w_m^k in MIW-PSO is not a fixed constant and changes continuously to balance the global and local search ability for the purpose of speeding up convergence and avoiding local optima.

Using the KL divergence [29], we define a fitness function to measure the distribution difference between the true SAW density distribution and the predicted SAW density distribution. Combining with (3) and (4), the fitness function can be written as follows:

$$F\left(E_m^k\right) = \sum_{a,b,c} P_{u-1}^{d+1}(a, b, c) \log \frac{P_{u-1}^{d+1}(a, b, c)}{\hat{P}_{u-1}^{d+1}(a, b, c)|_m^k}. \tag{7}$$

A nonnegative F is equal to 0 only if $P = \widehat{P}$, where the predicted density distribution is the same as the actual density distribution according to (7). When P = 0 or $\hat{P} = 0$, we add a very small number epsilon = 1.e − 12 to P or $\widehat{P}$, which will not affect the results. Here, $\hat{P}_{u-1}^{d+1}(a, b, c)|_m^k$ represents the calculated value at the k-th iteration for the m-th particle of the swarm.

Based on the aforementioned definitions and formulas, the weight for the m-th particle at the k-th iteration can be deduced as

$$w_m^k = \frac{1}{\left(1 + e^{-\Delta F}\right)}, \tag{8}$$

$$\Delta F = F\left(E_m^{k-1}\right) - F\left(E_m^{k-2}\right), \tag{9}$$

where the value of w is limited to the range of $[0, 1]$, and it is randomly generated when k is less than 2. Meanwhile, ΔF denotes the change in the fitness value. When ΔF is relatively large, its weight increases while also increasing the global search ability. When the value of ΔF is relatively small, this leads to an enhancement in the local search capability.

C. SAW Discovery Algorithm

The SAW discovery procedure based on 3D-KDE with MIW-PSO is presented in Algorithm 1. Considering the dependence of the SAW density distributions on time, the 3D-KDE-based model is designed to transform the space-time SAW data into 3D density distributions, which can reveal the variations of the aggregation effect. Based on the assumption that the SAW of the current day is related to historical days of the current week and the current day of the previous week, the relevance is described by the weight coefficient parameter. We use the MIW-PSO algorithm to efficiently search for the optimal parameter. After a certain number of iterations, the weight coefficients are altered to achieve better results regarding the fitness function until the end of the optimization. Combining the historical SAW density distribution with the optimal parameter, the predicted density estimation of the predicted day (i.e., $\hat{P}_u^{d+1}$) can be obtained.

Algorithm 1 SAW Discovery Based on 3D-KDE With MIW-PSO

Input: SAW dataset obtained from private car trajectory data
Output: The predicted density distribution of P_u^{d+1}, namely, $\hat{P}_u^{d+1}$

Set the initial value h_t, h_s and the k kernel function; meanwhile, set a group (dx, dy, dz), determine population of particle pairs (C^1, C^2), random position V_m and E_m; and set the initial parameters N_{maxiter}, N_{size}, u, d, w, $k = 1$.
Obtain the density distribution P on every day based on the 3D Kernel Density Estimation model.
while $k <= N_{\max iter}$ **do**
  for $m = 1$ to N_{size} **do**
    Calculate the fitness value $F\left(E_m^k\right)$ of the new particle based on (7).
    if $F\left(E_m^k\right)$ is better than $F\left(lbp_m^k\right)$ **then**
      Set E_m^k to be lbp_m^k
    end if
    if $F\left(E_m^k\right)$ is better than $F\left(gbp_g\right)$ **then**
      Set E_m^k to be gbp_g
    end if
    Compute w_m^k according to (8)
  end for
  if F is not relatively changed **then**
    Output the optimal E set
  else
    Let $k = k + 1$
  end if
end while
Provide the optimal E set;
Compute $\hat{P}_u^{d+1}$ based on (4).

IV. Experimental Results and Analysis

In this section, we conduct experiments based on the real-world trajectory data to evaluate the performance of the SAW prediction. First, we give a brief introduction of the private car trajectory data that we have collected from real urban environments. Then, we retrieve the SAW points from the trajectory data. Finally, we conduct a comparative study by applying the proposed method and current methods to the SAW data. In addition to the KL divergence, we evaluate the performance in terms of MAE and RMSE for some fixed sampling voxels, which are expressed as follows:

$$MAE = \frac{1}{N}\sum_{a,b,c}\left|\hat{P}_{a,b,c} - P_{a,b,c}\right|, \tag{10}$$

$$RMSE = \sqrt{\frac{1}{N}\sum_{a,b,c}(\hat{P}_{a,b,c} - P_{a,b,c})^2}. \tag{11}$$

Based on (3), $P_{a,b,c}$ and $\hat{P}_{a,b,c}$ denote the true SAW density and the predicted SAW density value for the space-time cube in (a, b, c) from the 3D region (see in Fig. 2). N is equal to $n_a \times n_b \times n_c$. When we calculate the MAE and RMSE at a specific moment, c is a fixed value. Hence, the N can be obtained as $n_a \times n_b$.

A. Private Car Trajectory Data

In our previous work [30], we presented a vehicle trajectory data collection method based on a low-cost on-board unit (OBU), which offers a feasible method for large-scale trajectory acquisition and is particularly suitable for private cars. We adopt the device in [30] to obtain the position of the vehicle and read the driving status information through the on-board diagnostics (OBD) interface. Moreover, this device can record the position and time when the vehicle starts and shuts off the engine. We have thus generated a large-scale trajectory dataset, for which the trajectory data of more than 50000 private cars were collected from two cities in China: Shenzhen and Shanghai. In particular, the trajectory point is taken as the SAW point when the vehicle stops at a specific location and shuts off the engine for over five minutes. In other words, we define that the time interval of SAW should be longer than five minutes; thereby, the SAW dataset can be retrieved from large-scale private car trajectories. This can rule out certain sudden flameout points caused by unexpected factors. We perform the experiments using the SAW data for five weeks (excluding weekends and public holidays) from Shenzhen and Shanghai. Specifically, as shown in Table I, we select the SAW data collected from the Luohu District, Shenzhen, from January 4, 2016 to February 5, 2016 and the SAW data from Pudong District in Shanghai from June 25, 2018 to July 27, 2018 to perform the experiments.

For the SAW density prediction, the training data and testing data are set up according to Fig. 3. For instance, in Fig. 3(a), we use the SAW density distributions of January 20, January 25 and January 26 with corresponding weights to predict the SAW density of January 27 (Wednesday). The SAW

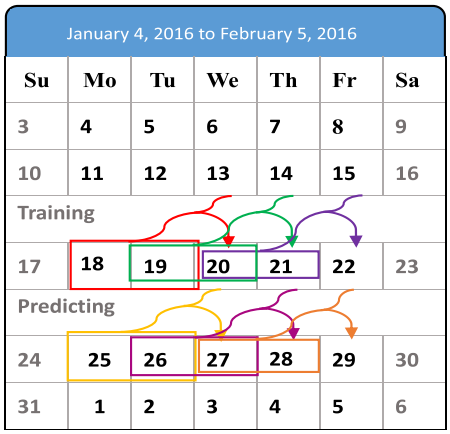

(a)

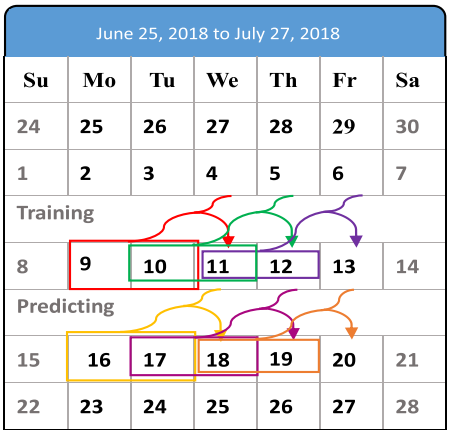

(b)

Fig. 3. SAW data for five weeks. (a) Shenzhen. (b) Shanghai.

TABLE I
THE SELECTED SAW DATA FROM SHENZHEN AND SHANGHAI

City	Five weeks (excluding weekends)	Latitude	Longitude
Luohu District, Shenzhen	Jan. 4, 2016 ∼ Feb. 5, 2016	22.50 ∼22.65	114.0 ∼114.2
Pudong District, Shanghai	Jun. 25, 2018 ∼ Jul. 27, 2018	31.10 ∼31.26	121.54∼121.68

data of January 13, January 18, January 19 and January 20 are applied to train the weight value for the prediction model. Specifically, we utilize the SAW data of this Monday and Tuesday as well as the last Wednesday with corresponding weight coefficients to predict the SAW density of the present Wednesday. In Fig. 3(b), we use the SAW densities of July 11, July 16 and July 17 to predict the SAW data of July 18 (Wednesday). For the training, the SAW data of July 9, July 10 and July 11 on the last week with the data from July 4 before the last Wednesday are used to train the weight parameter. In a similar manner, we can obtain the predicted density distributions of every Wednesday, Thursday, and Friday. Finally, we adopt the expectation maximization (EM) algorithm [31] and Voronoi method [22] for the comparative study.

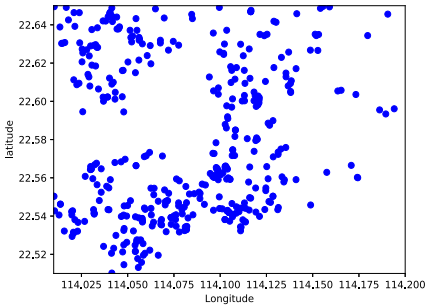

Fig. 4. Original SAW data from Luohu District, Shenzhen, 8:00 on January 27, 2016.

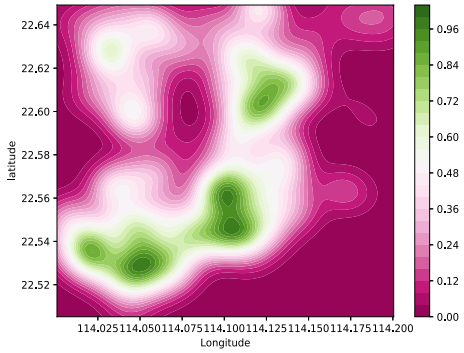

Fig. 5. Density estimation of SAW data from Luohu District, Shenzhen, 8:00 on January 27, 2016.

B. Results and Evaluation

Fig. 4 presents the original SAW points at 8:00 on January 27, 2016 for Luohu District, Shenzhen. Fig. 5 presents the results of the density distribution of the SAW behaviors, in which we normalize the density value to within [0,1] to avoid stretching effects. The bar graph on the right in Fig. 5 is used to describe the varying of the SAW density. The deep green denotes an area with a high SAW density, which indicates the aggregation effect and the forming of a hot zone. The deep red represents a low SAW density for the corresponding areas.

To illustrate the evolution of SAW, we plot the dynamic SAW density at three special moments, 8:00, 12:00 and 19:00, which are given in Fig. 6. Given the work schedules and lifestyles characterizing the Luohu District of Shenzhen, China, 8:00 is considered as rush hour; thus, we observe several aggregation areas, and hence, hot zones are forming. At 12:00, people go out for lunch, and most of them walk because they would not choose a far-off location. Furthermore, we can see that the degree of the aggregation effect decreases since the SAW density in the aggregation area at 12:00 is smaller than that at 8:00. Note that the rush hour in the afternoon is over by approximately 19:00 because it usually takes place from 17:30 to 18:30. As a result, the traffic situation is acceptable, and the SAW density is relatively low in the beginning of the evening (i.e., 19:00). In a word, the traffic congestion in the selected area has been greatly alleviated, and the aggregation effect has been lessened when comparing to that in the daytime.

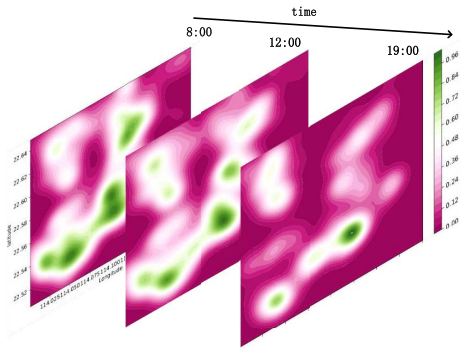

Fig. 6. Dynamic SAW at 8:00, 12:00 and 19:00 in Shenzhen.

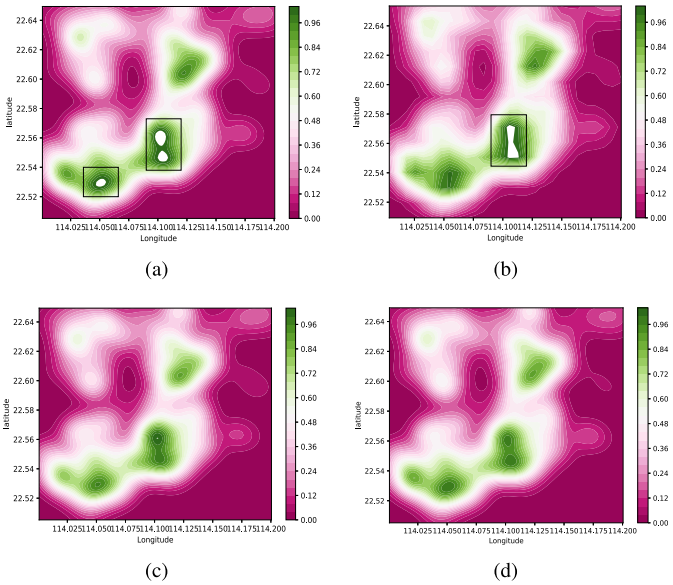

Fig. 7. The predicted SAW density distribution at 8:00 on January 27, 2016 in Shenzhen. (a) EM. (b) Voronoi. (c) Proposed. (d) True.

Fig. 7 presents the performance comparison of the predicted density distributions at 8:00, January 27, 2016 in Shenzhen, in which Fig. 7(a), Fig. 7(b) and Fig. 7(c) show the results generated by EM, Voronoi and the proposed method, respectively. It can be observed that the proposed method provides higher prediction performance since the predicted results better match the true SAW data, as shown in Fig. 7(d). In Fig. 7(a) and Fig. 7(b), it is obvious that the EM and Voronoi methods generate prediction errors, especially in locations where the SAW density is high (as shown in the black boxes). Moreover, the result of the Voronoi method is not smooth and is overly abrupt since the division of time and space makes it ignore density changes in neighboring spatio-temporal cubes [32].

Fig. 8 and Fig. 9 present the results of the SAW density prediction at 12:00 and 19:00, respectively, on January 27, 2016 for Shenzhen. In Fig. 8, it is shown that the density distributions under the three methods are roughly the same when comparing to that at 8:00 (see Fig. 7). The reasons behind this are as follows. Many people, who are living in various parts of the city, drive from home in the morning and head to their destinations, which are likely places of work such as the several aggregation areas shown in

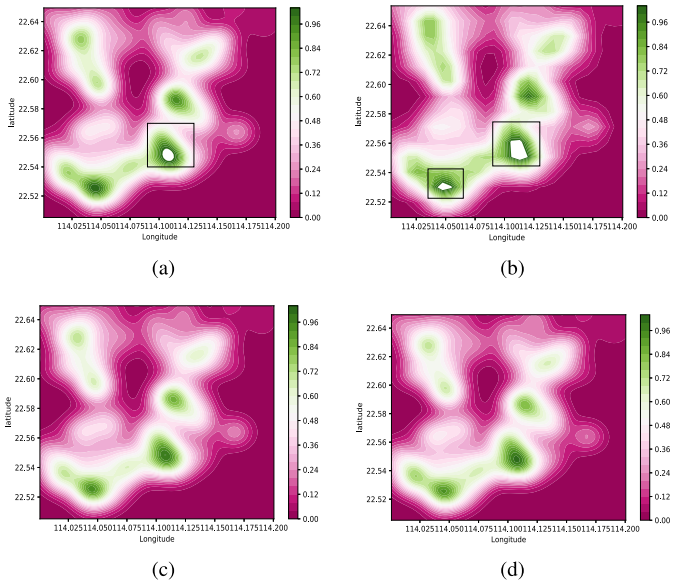

Fig. 8. The predicted SAW density distribution at 12:00 on January 27, 2016 in Shenzhen. (a) EM. (b) Voronoi. (c) Proposed. (d) True.

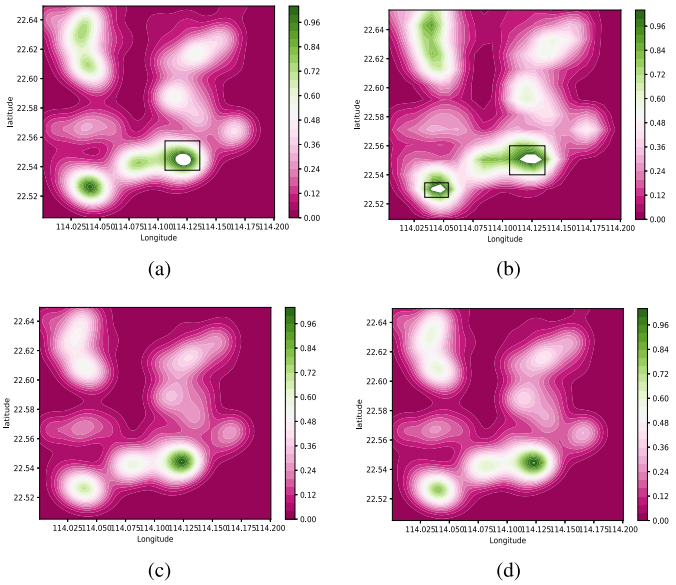

Fig. 9. The predicted SAW density distribution at 19:00 on January 27, 2016 in Shenzhen. (a) EM. (b) Voronoi. (c) Proposed. (d) True.

Fig. 7 and Fig. 8. Once these people reach these places, they stop their cars. As a result, by studying the SAW density distribution, we can observe that the SAW data reflect the aggregation effect, which leads to the formation of hot zones. In most cases, people, i.e., the private car drivers, do not drive in the daytime until they get off work and leave from their places of work. Therefore, the SAW density distributions at 8:00 and 12:00 are similar. Based on Fig. 9, we determine that an obvious change in SAW density at 19:00 occurs. On the one hand, the number of hot zones is decreasing; on the other hand, the degree of the aggregation effect is diminishing. This is because people drive and leave these areas; therefore, the SAW behaviors are reduced. The varying of the SAW behaviors is also supported by Fig. 6.

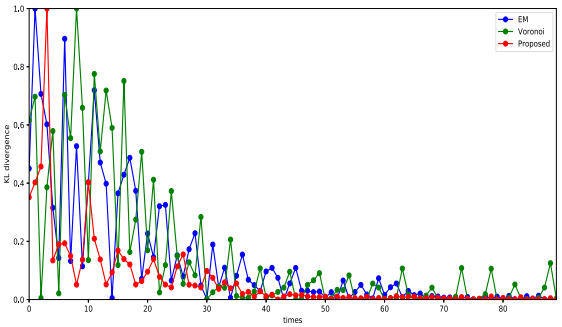

Fig. 10. KL divergence based on the SAW data in Shenzhen.

TABLE II

PREDICTION PERFORMANCE AT 8:00, 12:00 AND 19:00 ON JANUARY 27, 2016 IN SHENZHEN

		KL-divergence	MAE	RMSE
8:00	Voronoi	17.91789	21.24674	25.15245
	EM	13.13064	16.63308	18.66753
	Proposed	**11.08826**	**14.13175**	**15.39162**
12:00	Voronoi	15.31573	19.15182	20.51350
	EM	12.08806	18.84925	19.83315
	Proposed	**9.65608**	**11.20995**	**15. 54376**
19:00	Voronoi	12. 02296	17.72518	19. 01642
	EM	8. 12026	15.81281	18. 20942
	Proposed	**7. 68024**	**13.56021**	**16. 26536**

When we examine the prediction performance from Fig. 8 and Fig. 9, the areas marked with black boxs in Fig. 8(a), Fig. 8(b), Fig. 9(a), and Fig. 9(b) present obvious prediction errors. In general, the proposed method can achieve a better performance and make the predicted density distribution closer to the true values, thereby better capturing the aggregation effect.

To further evaluate the performance of the proposed method, we adopt three metrics, the KL divergence, MAE and RMSE, to conduct a quantitative study on the SAW density prediction. Fig. 10 gives the results of the normalized KL divergence, in which '0' represents that the actual and predicted values are the same and '1' indicates that the predicted value is far from the actual value. Compared with the EM method and the Voronoi method, our proposed method can more quickly converge to the real SAW density distribution.

Table II presents the prediction performance based on the SAW data from Shenzhen at 8:00, 12:00 and 19:00. The proposed method achieves smaller KL divergence, RMSE and MAE when comparing with the EM method and Voronoi method. For instance, at the 8:00 rush hour, the percentage improvement of the three metrics can be found to be 61.59%, 50.35%, and 63.42% when comparing to the Voronoi method. It can also be observed from Fig. 7 that the SAW density predicted by the Voronoi method has a larger deviation. Moreover, the percentage improvements of the KL divergence, MAE and RMSE under the proposed method are 18.42%, 17.70%, and 21.28%, respectively, over the EM method. According to Table III, in which the average prediction performance for

TABLE III

AVERAGE PREDICTION PERFORMANCE FOR THREE DAYS IN SHENZHEN

		KL-divergence	MAE	RMSE
Wednesday	Voronoi	30.11867	34.20852	36.09362
	EM	27.49882	29.14538	33.68527
	Proposed	**23.75764**	**27.05421**	**31.76027**
Thursday	Voronoi	27.85773	32.82082	35.14306
	EM	23.92361	25.61425	32.31732
	Proposed	**21.12608**	**22.17628**	**26.75253**
Friday	Voronoi	29.35976	31.71552	33.24373
	EM	26.12608	24.35976	30.86269
	Proposed	**20.91178**	**22.85284**	**25.30423**

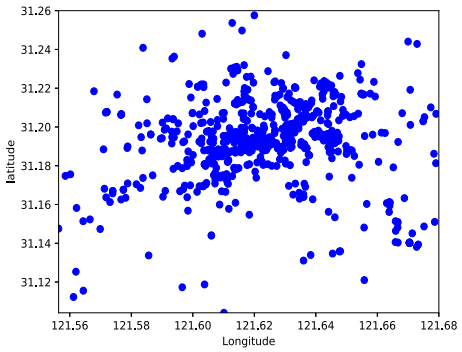

Fig. 11. Original SAW data from Pudong District, Shanghai at 8:00 on July 18, 2018.

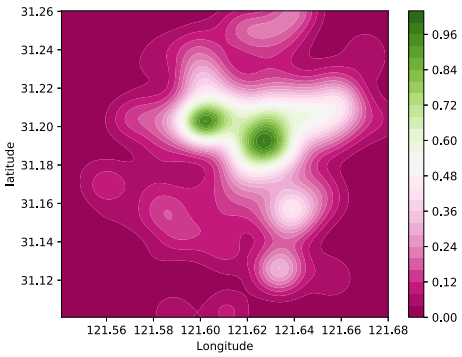

Fig. 12. Density estimation of SAW data from Pudong District, Shanghai at 8:00 on July 18, 2018.

Wednesdays, Thursdays and Fridays during three weeks is given, our proposed method obtains a better performance than the EM method and the Voronoi method.

Additionally, we collected SAW data for Pudong District in Shanghai from June 25, 2018 to July 27, 2018. Fig. 11 and Fig. 12 present the raw SAW points at 8:00 on July 18 and the corresponding density estimation, respectively. Fig. 13 illustrates the dynamic SAW density at 8:00, 12:00 and 19:00.

Fig. 14 and Fig. 15 give the SAW density prediction performance at 8:00 and 19:00, respectively. It can be found that the proposed method generates better density distributions than the comparative methods. Especially in the high-density region (marked by black box), prediction errors are found under the EM and Voronoi methods, whereas the proposed

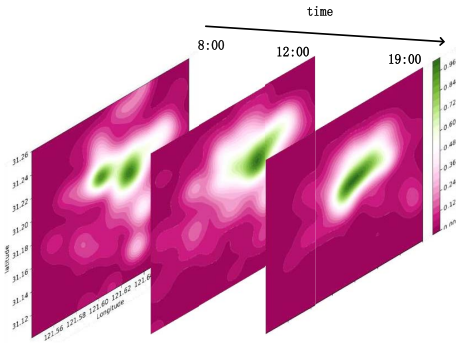

Fig. 13. Dynamic SAW at 8:00, 12:00 and 19:00 in Shanghai.

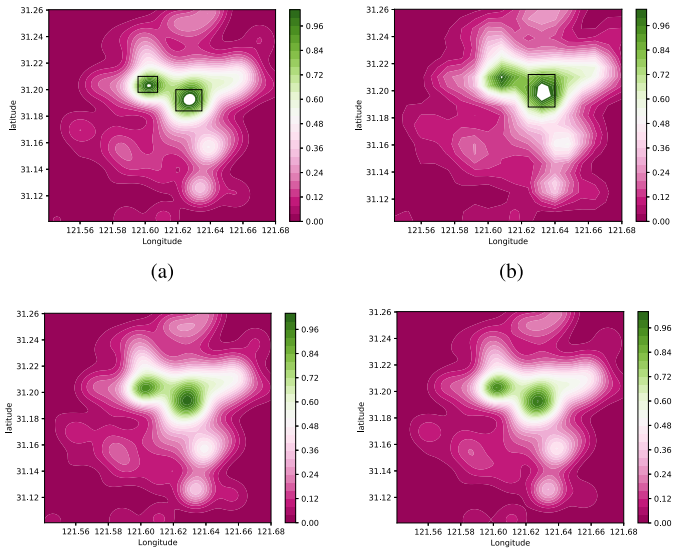

Fig. 14. The predicted SAW density distribution at 8:00 on July 18, 2018 in Shanghai. (a) EM. (b) Voronoi. (c) Proposed. (d) True.

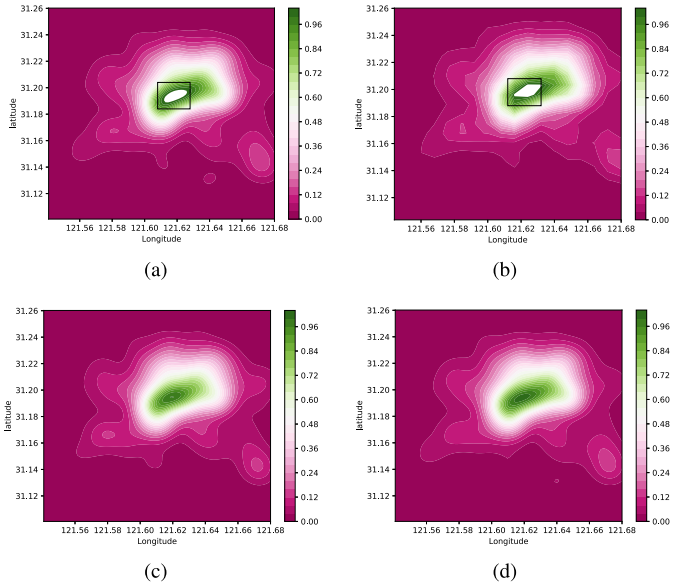

Fig. 15. The predicted SAW density distribution at 19:00 on July 18, 2018 in Shanghai. (a) EM. (b) Voronoi. (c) Proposed. (d) True.

method can perfectly match the true density distribution. Moreover, the results from Fig. 14 and Fig. 15 demonstrate the formation and disappearance of hot zones. A similar

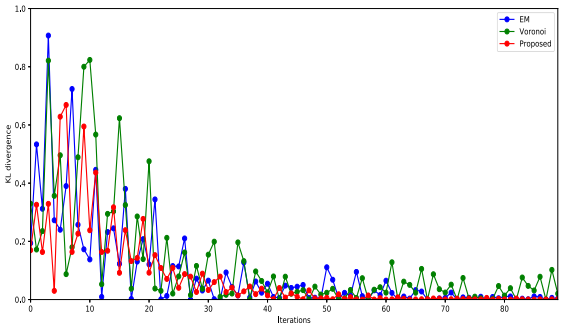

Fig. 16. KL divergence based on the SAW data in Shanghai.

TABLE IV

PREDICTION PERFORMANCE AT 8:00, 12:00 AND 19:00 ON JULY 18, 2018 IN SHANGHAI

		KL-divergence	MAE	RMSE
8:00	Voronoi	15.95101	21.52673	24.88549
	EM	13.52873	18.90408	21.58048
	Proposed	**10.32723**	**11.41692**	**18.47613**
12:00	Voronoi	12.25992	19.93397	23.18637
	EM	9.97025	17.16108	18.98582
	Proposed	**8.01226**	**14.01049**	**15.54376**
19:00	Voronoi	10.97308	15.28756	17.07059
	EM	7.96865	13.95238	16.14476
	Proposed	**6.30653**	**12.20650**	**14.63078**

TABLE V

AVERAGE PREDICTION PERFORMANCE FOR THREE DAYS IN SHANGHAI

		KL-divergence	MAE	RMSE
Wednesday	Voronoi	28.36919	30.94658	32.41864
	EM	28.30053	28.95145	31. 94923
	Proposed	**25.59197**	**27.29676**	**30. 39564**
Thursday	Voronoi	21.34908	26.43071	28.37552
	EM	20.48389	24.94791	27. 41720
	Proposed	**18.38759**	**21.50142**	**25. 95322**
Friday	Voronoi	25.42841	23.39162	26.52385
	EM	19.98551	22.98507	25.41031
	Proposed	**13. 96782**	**19. 96251**	**20. 95808**

phenomenon can be observed in Fig. 7, Fig. 8 and Fig. 9 when we study the results from Shenzhen. In a word, the SAW density changes over time, it gives rise to aggregation effects, and it vividly reflects peoples' daily lives.

Fig. 16 illustrates the KL divergence when we conduct experiments based on the data from Shanghai. It is evident that our proposed method can increase the convergence speed and achieve higher prediction accuracies. However, the EM and Voronoi methods show relatively large fluctuations during 100 iterations. Our proposed method converges to the true SAW density in fewer than 50 iterations.

Table IV presents the performance comparison for the EM method, Voronoi method and proposed method at 8:00, 12:00 and 19:00 on 18, 2018 in Shanghai. Table V presents the average prediction performance for three days based on

the SAW data from Shanghai. The results in Table IV show that the errors for the EM method and Voronoi method are relatively large at 8:00. Our method obtains an improvement in term of the three criteria of up to 54.46%, 88.55%, and 34.69% when compared to the Voronoi method. In addition, based on the results in Table V, our proposed method outperforms the comparison methods.

V. Conclusions

In this paper, to elucidate upon the time-varying aggregation effect, we propose a 3D-KDE based prediction model to characterize the dynamic spatiotemporal aggregation effect, which stems from the inherent relationship between the present SAW density and the future SAW aggregation. We conduct experiments based on real-world large-scale private car SAW data. The experimental results demonstrate that our proposed method outperforms current methods according to three criteria: the KL divergence, MAE and RMSE. Furthermore, we clearly observe the formation and disappearance of the aggregation effect during the experiments, which validates that the SAW behavior is of special significance to characterizing the dynamic aggregation effect. Summarizing, the current work on trajectory data focuses on floating cars and seldom consider private cars and their SAW behavior; our work attempts to fill this gap and bring a new perspective for studying aggregation effects based on large-scale private car trajectory data. In the future, we will integrate our approach with urban models to further explore human travel activities and the evolution of traffic flow.

Acknowledgment

The authors would like to thank Mr. Zhiwen Zhou and MapGoo Technology Co. Ltd for their support of our research work. The authors also appreciate the anonymous reviewers for their valuable suggestions on this paper.

References

[1] N. S. Wigginton, J. Fahrenkamp-Uppenbrink, B. Wible, and D. Malakoff, "Cities are the future," *Science*, vol. 352, no. 6288, pp. 904–905, 2016.

[2] G. Pan, G. Qi, W. Zhang, S. Li, Z. Wu, and L. T. Yang, "Trace analysis and mining for smart cities: Issues, methods, and applications," *IEEE Commun. Mag.*, vol. 51, no. 6, pp. 120–126, Jun. 2013.

[3] Z. Xiao *et al.*, "Spectrum resource sharing in heterogeneous vehicular networks: A noncooperative game-theoretic approach with correlated equilibrium," *IEEE Trans. Veh. Technol.*, vol. 67, no. 10, pp. 9449–9458, Oct. 2018.

[4] S. Chen, Z. Liu, and D. Shen, "Modeling social influence on activity-travel behaviors using artificial transportation systems," *IEEE Trans. Intell. Transp. Syst.*, vol. 16, no. 3, pp. 1576–1581, Jun. 2015.

[5] L. Xiang, M. Gao, and T. Wu, "Extracting stops from noisy trajectories: A sequence oriented clustering approach," *ISPRS Int. J. Geo-Inf.*, vol. 5, no. 3, p. 29, 2016.

[6] A. L. Alfeo, M. G. C. A. Cimino, S. Egidi, B. Lepri, and G. Vaglini, "A stigmergy-based analysis of city hotspots to discover trends and anomalies in urban transportation usage," *IEEE Trans. Intell. Transp. Syst.*, vol. 19, no. 7, pp. 2258–2267, Jul. 2018.

[7] Z. Feng and Y. Zhu, "A survey on trajectory data mining: Techniques and applications," *IEEE Access*, vol. 4, pp. 2056–2067, 2017.

[8] Y. Zheng, L. Capra, O. Wolfson, and H. Yang, "Urban computing: Concepts, methodologies, and applications," *ACM Trans. Intell. Syst. Technol.*, vol. 5, no. 3, 2014, Art. no. 38.

[9] C. N. S. Bureau, *China Statistical Yearbook 2016*. Beijing, China: China Statistical Publishing House, 2016.

[10] X. J. Kong *et al.*, "Mobility dataset generation for vehicular social networks based on floating car data," *IEEE Trans. Veh. Technol.*, vol. 67, no. 5, pp. 3874–3886, May 2018.

[11] D. Wang, Q. Liu, Z. Xiao, J. Chen, Y. Huang, and W. Chen, "Understanding travel behavior of private cars via trajectory big data analysis in urban environments," in *Proc. IEEE DataCom*, Orlando, FL, USA, Nov. 2017, pp. 917–924.

[12] J. Shang, Y. Zheng, W. Tong, E. Chang, and Y. Yu, "Inferring gas consumption and pollution emission of vehicles throughout a city," in *Proc. ACM SIGKDD Int. Conf. Knowl. Discovery Data Mining*, 2014, pp. 1027–1036.

[13] G. Goulet-Langlois, H. N. Koutsopoulos, Z. Zhao, and J. Zhao, "Measuring regularity of individual travel patterns," *IEEE Trans. Intell. Transp. Syst.*, vol. 19, no. 5, pp. 1583–1592, May 2018.

[14] F. Zhang, B. Jin, Z. Wang, H. Liu, J. Hu, and L. Zhang, "On geocasting over urban bus-based networks by mining trajectories," *IEEE Trans. Intell. Transp. Syst.*, vol. 17, no. 6, pp. 1734–1747, Jun. 2016.

[15] B. Barabino, M. Di Francesco, and S. Mozzoni, "Regularity analysis on bus networks and route directions by automatic vehicle location raw data," *IET Intell. Transport Syst.*, vol. 7, no. 4, pp. 473–480, Dec. 2013.

[16] J. Lv, Q. Li, Q. Sun, and X. Wang, "T-CONV: A convolutional neural network for multi-scale taxi trajectory prediction," in *Proc. IEEE Int. Conf. Big Data Smart Comput. (BigComp)*, Jan. 2018, pp. 82–89.

[17] M.-F. Chiang, E.-P. Lim, W.-C. Lee, and A. T. Kwee, "BTCI: A new framework for identifying congestion cascades using bus trajectory data," in *Proc. IEEE Int. Conf. Big Data (Big Data)*, Dec. 2017, pp. 1133–1142.

[18] L. Zeng *et al.*, "A new method based on pca contribution factors for road hotspot cause analysis," in *Proc. IEEE SmartWorld, Ubiquitous Intell. Comput., Adv. Trusted Computed, Scalable Comput. Commun., Cloud Big Data Comput., Internet People Smart City Innov. (SmartWorld/SCALCOM/UIC/ATC/CBDCom/IOP/SCI)*, Aug. 2017, pp. 1–5.

[19] C. Wan, Y. Zhu, J. Yu, and Y. Shen, "SMOPAT: Mining semantic mobility patterns from trajectories of private vehicles," *Inf. Sci.*, vol. 429, pp. 12–25, Mar. 2018. [Online]. Available: http://www.sciencedirect.com/science/article/pii/S0020025517302323

[20] S. Qiao, N. Han, W. Zhu, and L. A. Gutierrez, "TraPlan: An effective three-in-one trajectory-prediction model in transportation networks," *IEEE Trans. Intell. Transp. Syst.*, vol. 16, no. 3, pp. 1188–1198, Jun. 2015.

[21] X. Wan, J. Wang, Y. Du, and Y. Zhong, "DBH-CLUS: A hierarchal clustering method to identify pick-up/drop-off hotspots," in *Proc. 15th IEEE/ACM Int. Symp. Cluster, Cloud Grid Comput.*, May 2015, pp. 890–897.

[22] Q. Man, D. Mingyi, and L. Yang, "Application of Voronoi diagrams and multiangle measurable image in the urban POI location and site generation," in *Proc. IET Int. Conf. Inf. Sci. Control Eng. (ICISCE)*, Dec. 2012, pp. 1–5.

[23] D. Liu *et al.*, "SmartAdP: Visual analytics of large-scale taxi trajectories for selecting billboard locations," *IEEE Trans. Vis. Comput. Graphics*, vol. 23, no. 1, pp. 1–10, Jan. 2017.

[24] Z. Wang, M. Lu, X. Yuan, J. Zhang, and H. van de Wetering, "Visual traffic jam analysis based on trajectory data," *IEEE Trans. Vis. Comput. Graphics*, vol. 19, no. 12, pp. 2159–2168, Dec. 2013.

[25] W. R. Tobler, "A computer movie simulating urban growth in the detroit region," *Econ. Geogr.*, vol. 46, pp. 234–240, Jun. 1970.

[26] S. Wang, J. Wang, and F.-L. Chung, "Kernel density estimation, kernel methods, and fast learning in large data sets," *IEEE Trans. Cybern.*, vol. 44, no. 1, pp. 1–20, Jan. 2014.

[27] B. W. Silverman, *Density Estimation for Statistics and Data Analysis*. London, U.K.: Chapman & Hall, 1998.

[28] J. Kennedy and R. Eberhart, "Particle swarm optimization," in *Proc. IEEE ICNN*, vol. 4. Nov./Dec. 1995, pp. 1942–1948.

[29] M. N. Do and M. Vetterli, "Wavelet-based texture retrieval using generalized Gaussian density and Kullback-Leibler distance," *IEEE Trans. Image Process.*, vol. 11, no. 2, pp. 146–158, Feb. 2002.

[30] Z. Xiao, P. Li, V. Havyarimana, G. M. Hassana, D. Wang, and K. Li, "GOI: A novel design for vehicle positioning and trajectory prediction under urban environments," *IEEE Sensors J.*, vol. 18, no. 13, pp. 5586–5594, Jul. 2018.

[31] A. Ganjavi, E. Christopher, C. M. Johnson, and J. Clare, "A study on probability of distribution loads based on expectation maximization algorithm," in *Proc. IEEE Power Energy Soc. Innov. Smart Grid Technol. Conf.*, Apr. 2017, pp. 1–5.

[32] N. Xia, C. Wang, Y. Yu, H. Du, C. Xu, and J. Zheng, "A path forming method for water surface mobile sink using Voronoi diagram and dominating set," *IEEE Trans. Veh. Technol.*, vol. 67, no. 8, pp. 7608–7619, Aug. 2018.

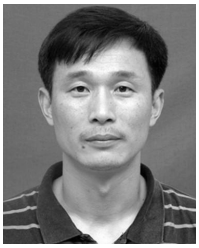

Dong Wang (M'15) received the B.S. and Ph.D. degrees in computer science from Hunan University, China, in 1986 and 2006, respectively. From 2004 to 2005, he was a Visiting Scholar with the University of Technology Sydney, Australia. Since 1986, he has been with Hunan University, where he is currently a Professor. His main research interests include network test and performance evaluation, wireless communications, and mobile computing.

Jiaojiao Fan received the B.S. degree from Nanchang University, China, in 2016. She is currently pursuing the M.S. degree in computer science and technology with Hunan University. Her research interests include intelligent transportation system and mobile computing.

Zhu Xiao (M'15) received the M.S. and Ph.D. degrees in communication and information system from Xidian University, China, in 2007 and 2010, respectively. From 2010 to 2012, he was a Research Fellow with the Department of Computer Science and Technology, University of Bedfordshire, U.K. He is currently an Associate Professor with the College of Computer Science and Electronic Engineering, Hunan University, China. His research interests include mobile computing, Internet of Vehicles, and big data mining.

Hongbo Jiang (M'08–SM'14) received the Ph.D. degree from Case Western Reserve University in 2008. He was a Professor at the Huazhong University of Science and Technology. He is currently a Full Professor with the College of Computer Science and Electronic Engineering, Hunan University. His research concerns computer networking, especially algorithms and protocols for wireless and mobile networks. He is serving as the Editor for the IEEE/ACM TRANSACTIONS ON NETWORKING, as the Associate Editor for the IEEE TRANSACTIONS ON MOBILE COMPUTING, and as the Associate Technical Editor for the *IEEE Communications Magazine*.

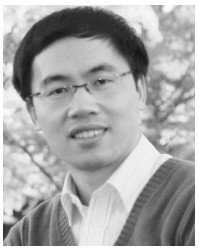

Hongyang Chen (M'11–SM'16) received the Ph.D. degree from The University of Tokyo. In 2009, he was a Visiting Researcher with the UCLA Adaptive Systems Laboratory, University of California at Los Angeles. His research interests include IoT, intelligent networking, location estimation and location-based service, and signal processing for communications. He served as an Editor for the IEEE TRANSACTIONS ON WIRELESS COMMUNICATIONS and as the Associate Editor for the IEEE COMMUNICATIONS LETTERS.

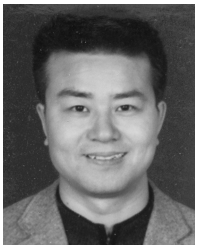

Fanzi Zeng received the Ph.D. degree in signal and information processing from Beijing Jiaotong University, Beijing, China, in 2005. Since 2005, he has been with the College of Computer Science and Electronic Engineering, Hunan University, Changsha, China, where he is currently a Professor. In 2009, he was with the Department of Electrical and Computer Engineering, Michigan Technological University, Houghton, MI, USA, as a Visiting Scholar. His current research focuses on cognitive radio technology and artificial intelligence.

Keqin Li (F'16) was an Intellectual Ventures endowed Visiting Chair Professor at the National Laboratory for Information Science and Technology, Tsinghua University, Beijing, China, from 2011 to 2014. He is currently a SUNY Distinguished Professor of computer science with The State University of New York. He is also a Distinguished Professor of the Chinese National Recruitment Program of Global Experts (1000 Plan) at Hunan University, China. He has published over 550 journal articles, book chapters, and refereed conference papers, and has received several best paper awards. His current research interests include parallel computing and high-performance computing, distributed computing, energy-efficient computing and communication, heterogeneous computing systems, cloud computing, big data computing, CPU-GPU hybrid and cooperative computing, multicore computing, storage and file systems, wireless communication networks, sensor networks, peer-to-peer file sharing systems, mobile computing, service computing, Internet of things and cyber-physical systems. He is currently serving or has served on the editorial boards of the IEEE TRANSACTIONS ON PARALLEL AND DISTRIBUTED SYSTEMS, the IEEE TRANSACTIONS ON COMPUTERS, the IEEE TRANSACTIONS ON CLOUD COMPUTING, the IEEE TRANSACTIONS ON SERVICES COMPUTING, and the IEEE TRANSACTIONS ON SUSTAINABLE COMPUTING.